Supporting Information

Morphology inherence from hollow MOFs to hollow carbon polyhedrons in preparing carbon-based electrocatalysts

Yuchen Pei,†[ab] Zhiyuan Qi,†[ab] Xinle Li,[ab] Raghu V. Maligal-Ganesh,[ab] Tian Wei Goh,[ab] Chaoxian Xiao,[a] Tianyu Wang[c] and Wenyu Huang[ab]*

[a] Department of Chemistry, Iowa State University, Ames, Iowa 50014, United States.
[b] Ames Laboratory, Department of Energy, Ames, Iowa 50014, United States.
[c] Department of Mechanical Engineering, Iowa State University, Ames, Iowa 50011, United States.
† These authors contribute equally.
* E-mail: whuang@iastate.edu

Experimental

1. Synthesis of ZIF-control and Cz-ZIF-control

50 mL 0.1 mol/L $M(NO_3)_2 \cdot 6H_2O$ (M = Zn and Co, Zn:Co = 1:1) methanol solution and 50 mL 0.8 mol/L 2-methyl imidazole methanol solution were prepared separately. Under magnetic stirring, the 2-methylimidazole solution was poured into Zn/Co solution and stirred for 2 hrs. The mixture solution was centrifuged, washed and dried in vacuum. After carbonization following the same procedure as that of HCPs, Cz-ZIF-control was obtained.

Table S1. ICP-MS and ICP-OES results.

samples	Co /wt.%	Zn /wt.%	Fe /wt.%	weight loss after carbonization /%
Hollow ZIF-67/8	11.4	18.6	-	-
HCPs	23.9	0.1	-	51.3
Core/shell ZIF-67/8	18.2	5.5	-	-
SCPs	41.3	< 0.1	-	57.7
Fe/hollow ZIF-67/8	16.3	27.8	-	-
1.0 wt.% Fe/HCPs	34.4	0.1	1.0	-
ZIF-control	12.3	9.6	-	-
Cz-ZIF-control	41.8	1.2	-	48.8
HCPs-etching	8.1	< 0.1	-	-
Fe-HCPs-etching	11.5	< 0.1	0.9	-

Table S2. Porosity summary of carbonized materials.

samples	HCPs	SCPs	Cz-ZIF-control
BET surface areas / $m^2 \cdot g^{-1}$	227	282	361
Mesoporous volume / $cm^3 \cdot g^{-1}$	0.47[a]	0.35[a]	0.60[c]
Microporous volume /$cm^3 \cdot g^{-1}$[b]	0.07	0.01	0

[a] BJH adsorption from 0.6-400 nm; [b] determined by the t-plot method; and [c] single point (< 291.8 nm) adsorption total pore volume of pores.

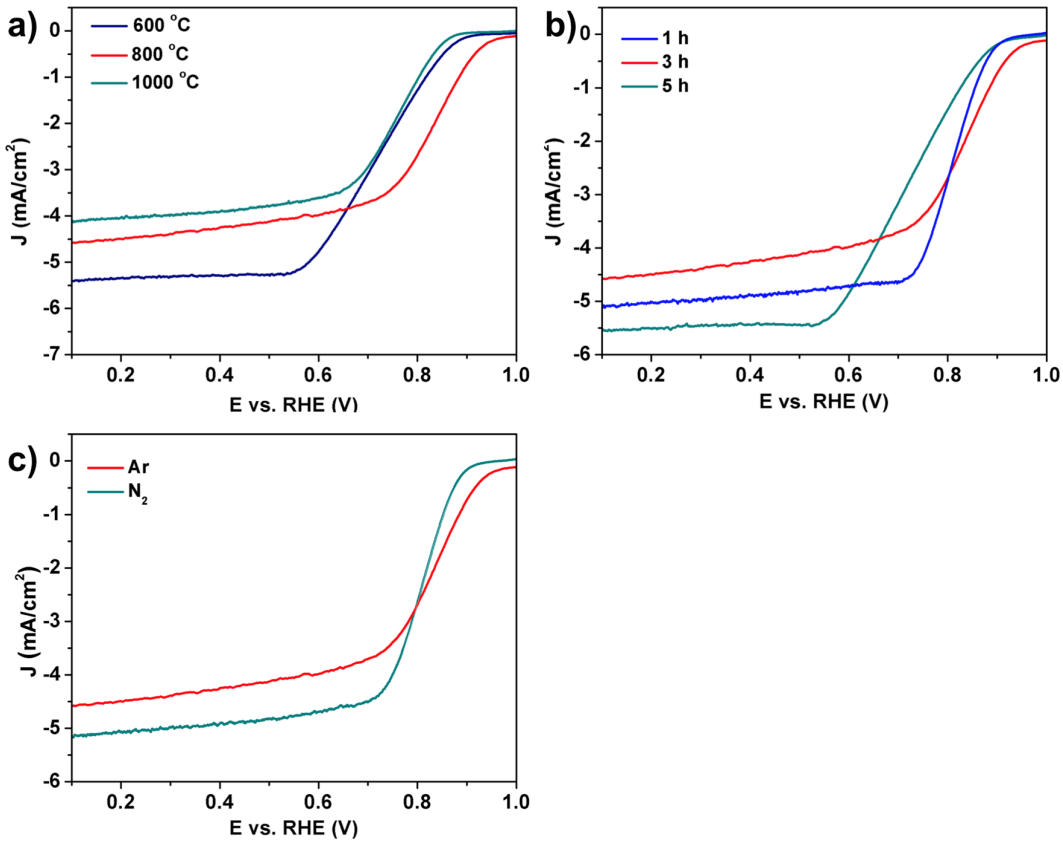

Figure S1. ORR performance of a) HCPs carbonized at 600, 800, and 1000 °C for 3 h in Ar; b) HCPs carbonized at 800 °C for 1, 3 and 5 h Ar; and c) HCPs carbonized at 800 °C for 3 h in Ar and N_2. In all conditions, HCPs prepared at 800 °C for 3 h have the best $E_{1/2}$. We did not evaluate the ORR performance of HCPs when employing 10% H_2/Ar, because most of the carbons in HCPs were removed/decomposed in the presence of H_2 at 800 °C.

Table S3. ORR summary of carbon catalysts with different synthesis conditions.

samples	$E_{1/2}$ (V)	E_{onset} (V)	$J_{limiting}$ (mA/cm^2) at 0.2 V	$J_{kinetic}$ (mA/cm^2) at 0.9 V
HCPs-3 h-800 °C-Ar	0.821	0.948	4.49	0.87
HCPs-3 h-600 °C-Ar	0.718	0.875	5.43	0.14
HCPs-3 h-1000 °C-Ar	0.751	0.859	4.02	0.047
HCPs-1 h-800 °C-Ar	0.807	0.896	5.02	0.22
HCPs- 5h-800 °C-Ar	0.722	0.887	5.51	0.19
HCP-3 h-800 °C-N_2	0.805	0.888	5.08	0.18

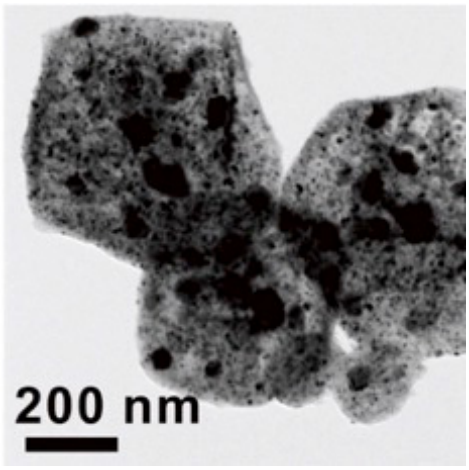

Figure S2. TEM image of Fe/HCPs.

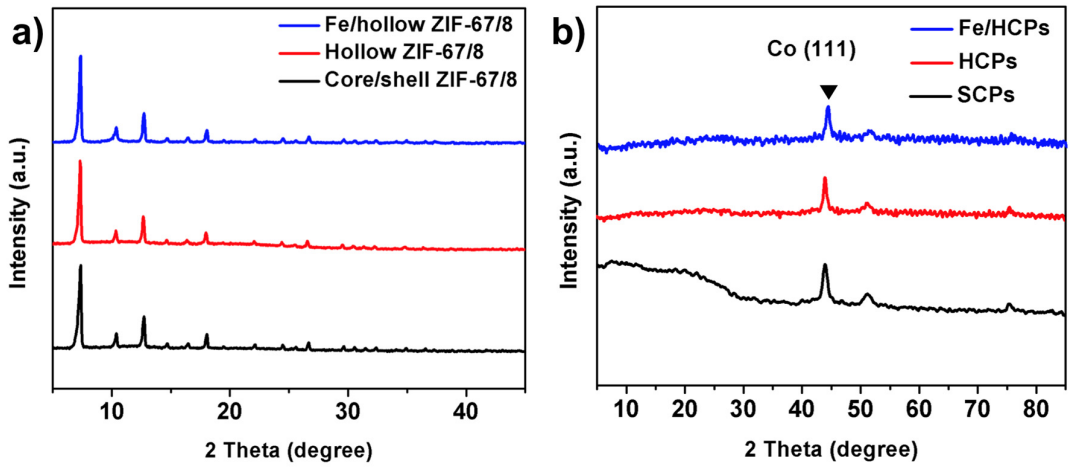

Figure S3. PXRD patterns of (a) parent ZIFs, and (b) HCPs, SCPs, and Fe/HCPs.

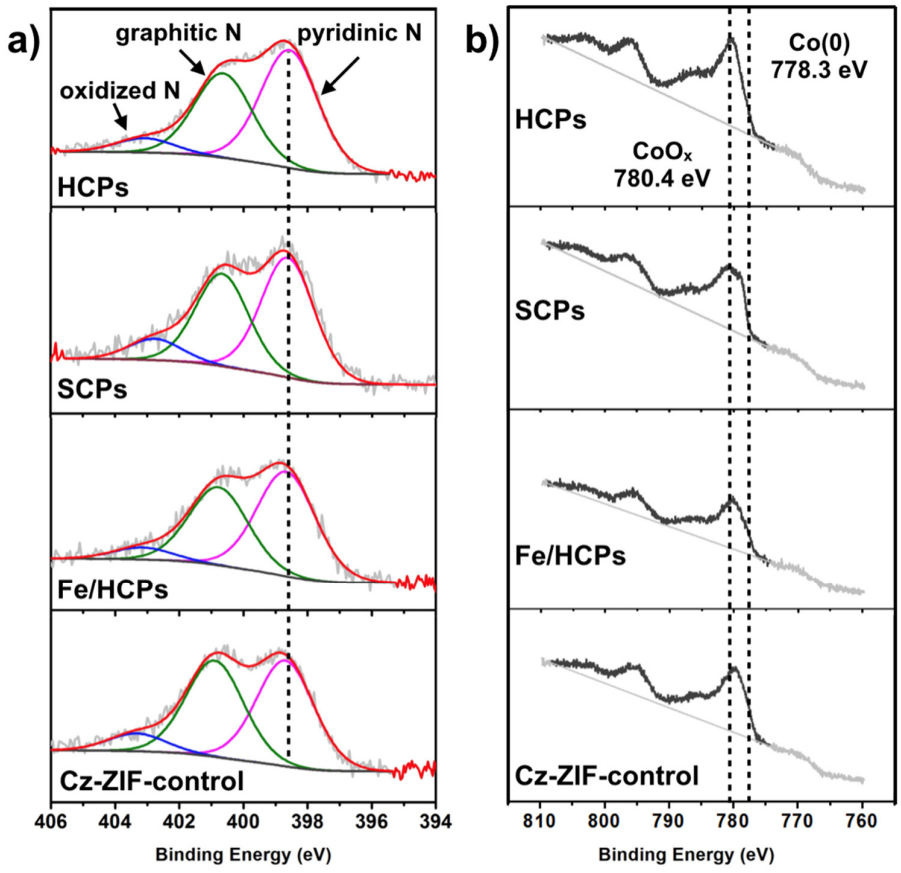

Figure S4. XPS spectra of HCPs, SCPs, Fe/HCPs and Cz-ZIF-control: (a) N 1s, and (b) Co 2p.

Table S4. XPS analysis of carbonized materials.

samples	N /%	Co /%	C /%	Zn /%	Fe /%
HCPs	6.7	2.2	81.9	0.1	-
SCPs	5.2	3.2	84.6	0.3	-
Fe/HCPs	5.6	2.2	83.2	0.1	trace
Cz-ZIF-control	4.7	2.2	88.2	-	-

N analysis	Pyridinic-N (398.6 ± 0.1 eV) /%	Graphitic-N (400.7 ± 0.2 eV) /%	Oxidized N (403.0 ± 0.3 eV) /%
HCPs	54.3	39.0	6.6
SCPs	51.2	39.6	9.1
Fe/HCPs	53.7	40.1	6.2
Cz-ZIF-control	48.0	43.8	8.1

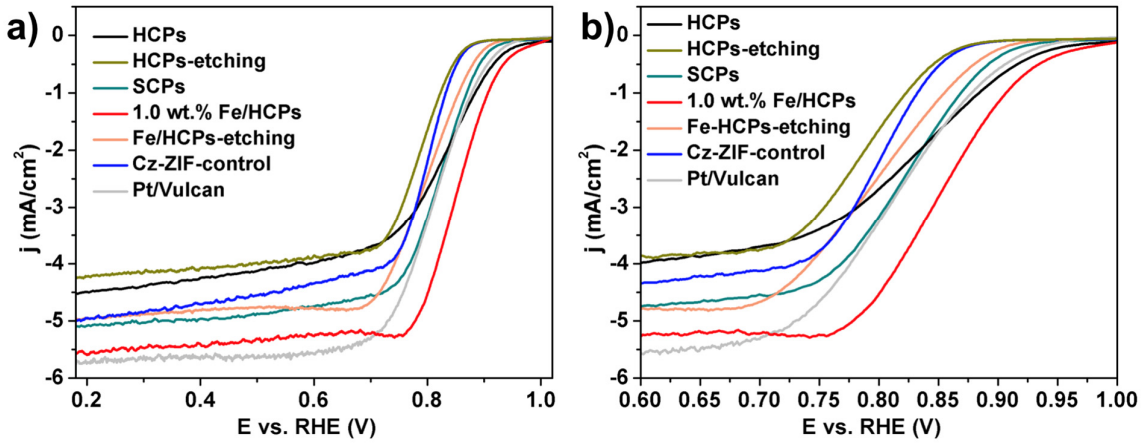

Figure S5. (a) ORR polarization curves of HCPs, HCPs-etching, SCPs, 1.0 wt.% Fe/HCPs, Fe/HCPs-etching, Cz-ZIF-control, and Pt/Vulcan commercial catalyst. (b) enlarged area of plot a) at the range from 0.65 V to 1.00 V.

Table S5. ORR summary of different carbon catalysts.

samples	$E_{1/2}$ (V)	E_{onset} (V)	$J_{limiting}$ (mA/cm^2) at 0.2 V	$J_{kinetic}$ (mA/cm^2) at 0.9 V
HCPs	0.821	0.948	4.49	0.87
SCPs	0.810	0.912	5.08	0.40
Fe/HCPs	0.850	0.960	5.59	1.47
HCPs-etching	0.784	0.869	4.22	0.096
Fe/HCPs-etching	0.799	0.900	4.96	0.26
Cz-ZIF-control	0.793	0.869	4.94	0.10
Pt/Vulcan	0.812	0.925	5.73	0.53

All the current densities were normalized by electrode geometric surface area. The kinetic current was calculated by $1/j = 1/j_{limiting} + 1/j_{kinetic}$.

Table S6. Literature summary of electro-catalytic results of carbon nanostructures in ORR.

samples	$E_{1/2}$ (V)	E_{onset} (V)	$J_{limiting}$ (mA/cm^2)[a]	Condition	Ref.
1:1 Fe-N/carbon nanoshell	0.85	0.98	5.0 at 0.2 V	0.1 M KOH	1
P-CNCo-20	0.85	0.93	5.8 at -0.6 V[b]	0.1 M KOH	2
MDC (Cz-ZIF-67)-750°C	~ 0.75	~ 0.95	~ 5.5 at 0.2 V	0.1 M $HClO_4$	3
Co@Co_3O_4/NC-1	0.80	~ 0.90	~ 4.4 at 0.2 V	0.1 M KOH	4
Hollow Fe_3C/C-700	0.83	1.05	~ 3.75 at 0.2 V	0.1 M KOH	5
N-MCNSs	~ 0.67	~0.82	~ 3.6 at -0.6 V [b]	0.1 M KOH	6
ZIF-67-900-AL	0.85	0.92	~ 5.2 at 0.4 V	0.1 M KOH	7
FeIM/ZIF-8	0.755	0.915	-	0.1 M KOH	8

[a] Rotation speed is 1600 rpm; [b] vs. Ag/AgCl.

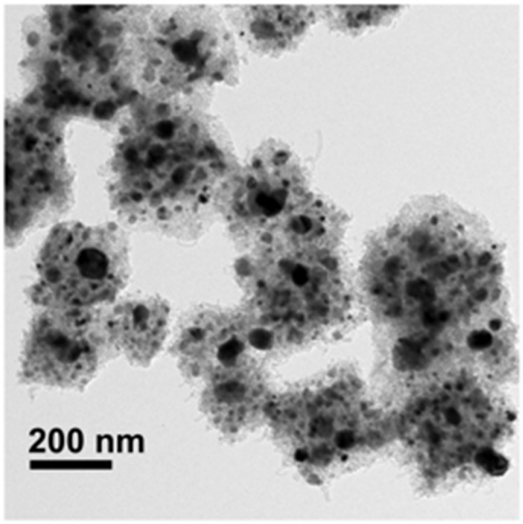

Figure S6. TEM image of Cz-ZIF-control. The Cz-ZIF-control was prepared by carbonizing the bimetallic ZIF-control using the mixture of Co and Zn precursors. This sample serves as a control catalyst to evaluate the electrochemical activity of HCPs and SCPs. The average size of Cz-ZIF-control is around 200-300 nm that is similar to that of HCPs and SCPs. The block morphology of Cz-ZIF-control is similar to the parent ZIFs, which evidences the morphology inherence as well. However, Cz-ZIF-control is not uniform due to that their parent ZIF precursor has random morphologies.

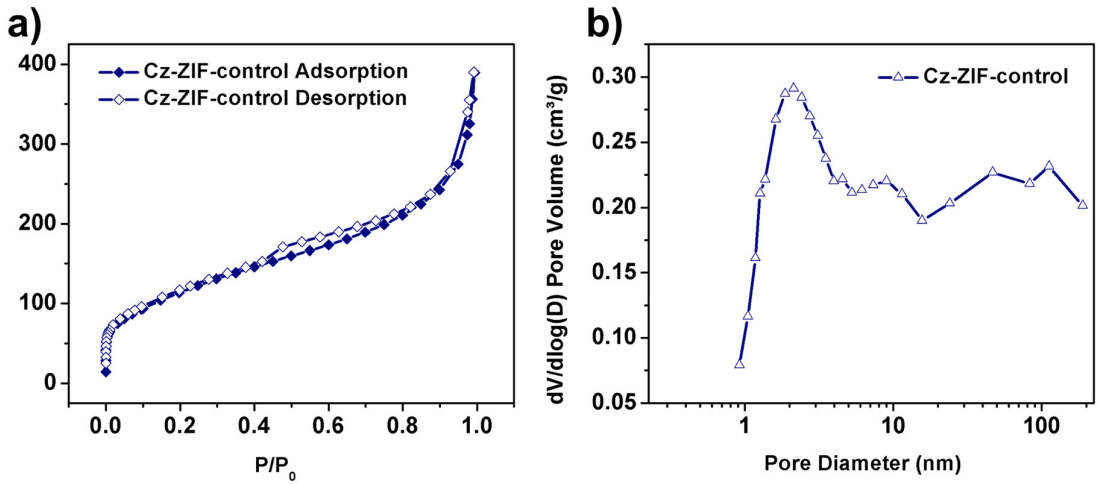

Figure S7. (a) N_2 physisorption isotherm and (b) pore size distribution of Cz-ZIF-control.

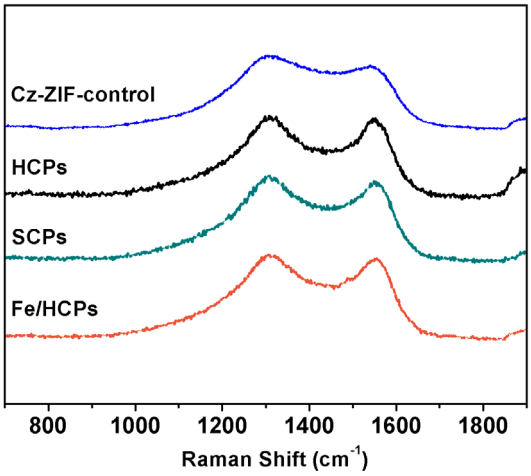

Figure S8. Raman spectra of HCPs, SCPs, Fe/HCPs, and Cz-ZIF-control.

Table S7. Raman spectra summary.

samples	D (cm^{-1})	I_D	G (cm^{-1})	I_G	I_D/I_G
HCPs	1345	6171	1587	6929	1.02
SCPs	1345	7363	1592	6756	1.09
Fe/HCPs	1344	11071	1590	10467	1.06
Cz-ZIF-control	1340	25151	1578	21159	1.19

All the carbon materials have two similar peaks around 1350 cm^{-1} and 1580 cm^{-1}, which are the D band and G band of graphitic carbon. The intensity ratio of D band and G band (I_D/I_G) is 1.02 for HCPs and 1.06 for Fe/HCPs, indicating these catalysts have similar defect degrees. The peaks positions of Cz-ZIF-control have slightly left shifts, and the I_D/I_G ratio is higher compared to that of HCPs and SCPs.

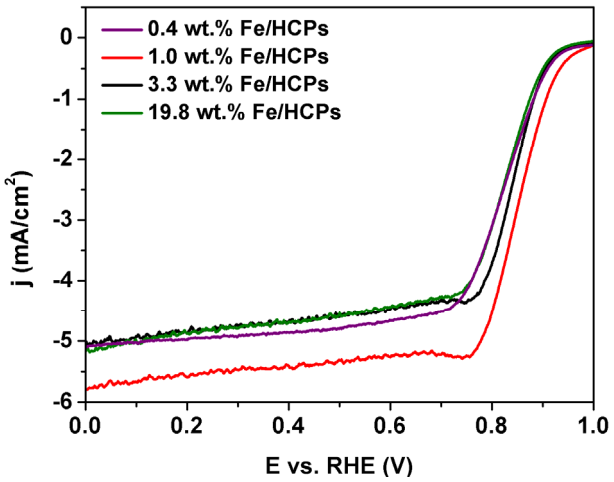

Figure S9. ORR polarization curves of Fe/HCPs with 0.4, 1.0, 3.3, and 19.8 wt.% Fe loading. The E_{onset} indicates that 1.0 wt.% Fe is the best loading under our reaction conditions. These actual loadings of Fe were measured by ICP-OES.

Table S8. ORR summary of carbon catalysts with different Fe loadings.

samples	$E_{1/2}$ (V)	E_{onset} (V)	$J_{limiting}$ (mA/cm^2) at 0.2 V	$J_{kinetic}$ (mA/cm$_2$) at 0.9 V
0.4 wt.% Fe/HCPs	0.824	0.937	4.98	0.74
1.0 wt.% Fe/HCPs	0.850	0.960	5.59	1.47
3.3 wt.% Fe/HCPs	0.840	0.929	4.87	0.67
19.8 wt.% Fe/HCPs	0.823	0.925	4.88	0.56

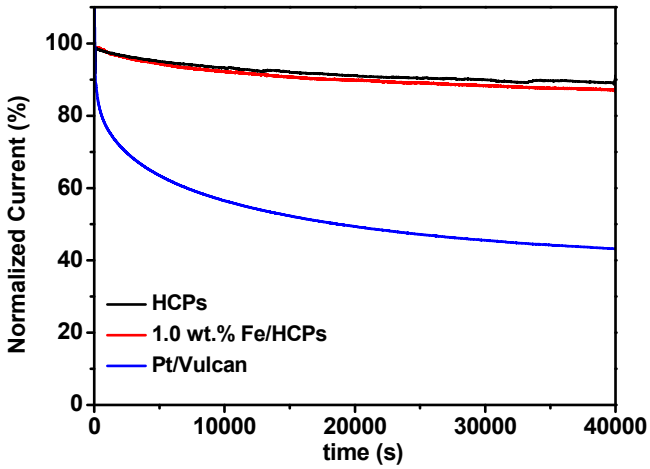

Figure S10. Chronoamperometric responses of HCPs, 1.0 wt.% Fe/HCPs, and commercial 20% Pt/Vulcan catalysts kept at 0.65 V vs. RHE in O_2 saturated 0.1 M KOH with a rotational speed of 400 rpm. All the current was normalized by the initial current, and the retained current was shown as a percentage.

Reference

1 Y. Wang, A. Kong, X. Chen, Q. Lin and P. Feng, *ACS Catal.*, 2015, **5**, 3887−3893.

2 Y. Z. Chen, C. Wang, Z. Y. Wu, Y. Xiong, Q. Xu, S. H. Yu and H. L. Jiang, *Adv. Mater.*, 2015, **27**, 5010−5016.

3 W. Xia, J. Zhu, W. Guo, L. An, D. Xia and R. Zou, *J. Mater. Chem. A*, 2014, **2**, 11606−11613.

4 A. Aijaz, J. Masa, C. Rosler, W. Xia, P. Weide, A. J. Botz, R. A. Fischer, W. Schuhmann and M. Muhler, *Angew. Chem. Int. Ed.*, 2016, **55**, 4087-4091.

5 Y. Hu, J. O. Jensen, W. Zhang, L. N. Cleemann, W. Xing, N. J. Bjerrum and Q. Li, *Angew. Chem. Int. Ed.*, 2014, **53**, 3675-3679.

6 T. Yang, J. Liu, R. Zhou, Z. Chen, H. Xu, S. Z. Qiao and M. J. Monteiro, *J. Mater. Chem. A*, 2014, **2**, 18139-18146.

7 X. Wang, J. Zhou, H. Fu, W. Li, X. Fan, G. Xin, J. Zheng and X. Li, *J. Mater. Chem. A*, 2014, **2**, 14064-14070.

8 D. Zhao, J. L. Shui, C. Chen, X. Chen, B. M. Reprogle, D. Wang and D. J. Liu, *Chem. Sci.*, 2012, **3**, 3200-3205.